Available online at www.sciencedirect.com
ScienceDirect
Polymer 48 (2007) 4628–4636
polymer
www.elsevier.com/locate/polymer

Synthesis and electro-optical properties of helical polyacetylenes carrying carbazole and triphenylamine moieties

Jinqing Qu, Yuji Suzuki, Masashi Shiotsuki, Fumio Sanda **, Toshio Masuda*

Department of Polymer Chemistry, Graduate School of Engineering, Kyoto University, Katsura Campus, Kyoto 615-8510, Japan

Received 19 March 2007; received in revised form 14 May 2007; accepted 5 June 2007
Available online 10 June 2007

Abstract

Novel chiral acetylene monomers bearing carbazole and triphenylamine groups, namely, (*S*)-3-butyn-2-yl 2-(9-carbazolyl)ethyl carbonate (**1**) and (*S*)-3-butyn-2-yl 4-(diphenylamino)benzoate (**2**) were synthesized, and polymerized with $Rh^{+}(nbd)[\eta^{6}\text{-}C_6H_5B^{-}(C_6H_5)_3]$ catalyst to give the corresponding polymers with moderate molecular weights (M_n 13.0×10^3 and 15.5×10^3) in good yields (86% and 88%). CD spectroscopic studies revealed that poly(**1**) and poly(**2**) took predominantly one-handed helical structure in $CHCl_3$. The helical structures of poly(**1**) and poly(**2**) were very stable against heating and addition of MeOH. The solution of poly(**1**) and poly(**2**) emitted fluorescence in 0.52% and 7.2% quantum yields, which were lower than those of the corresponding monomers **1** and **2** (22.5% and 76.5%). The cyclic voltammograms of the polymers indicated that the oxidation potentials of the polymers were lower than those of the monomers. The polymers showed electrochromism and changed the color from pale yellow to pale blue by application of voltage, presumably caused by the formation of polaron at the carbazole and triphenylamine moieties. The onset temperatures of weight loss of poly(**1**) and poly(**2**) were 225 and 270 °C under air.

Keywords: Carbazole; Helical polymer; Polyacetylene

1. Introduction

Recently, much attention has been paid to carbazole and triphenylamine derivatives because they are promising candidates for photoluminescence and electroluminescence materials [1]. Polymers containing carbazole or triphenylamine moieties in the main chain or side chain have been widely studied because of their unique properties, which allow them to be applied to various photonic materials including photoconductive, electroluminescent, and photorefractive materials [2–4]. Meanwhile, substituted polyacetylenes exhibit unique properties such as semiconductivity, nonlinear optical property, and high gas permeability based on the conjugated main chain and rigid molecular structure [5]. Helical polyacetylenes gather interest not only from the view point of synthesis and properties [6], but also from practical application, because they exhibit useful functions resulting from the regulated secondary structure, which include chiral discrimination and catalytic activity for asymmetric synthesis [7]. Incorporation of carbazole and triphenylamine into helical polyacetylenes possibly leads to the development of novel functional polymers based on synergistic actions of carbazole and triphenylamine with conjugated helical main chain. These polymers may form helical carbazole strands as well as a helical polyacetylene main chain, leading to unique electronic and photonic functions besides chiroptical properties.

We have reported the synthesis of poly(2-ethynylcarbazole) derivatives carrying chiral pendent carbamate groups [8,9]. These polymers take helical conformation and exhibit electrochemical and liquid crystalline properties. We have also reported that introduction of amino acid between the polyacetylene backbone and carbazole is effective to induce a helical structure, keeping electrochemical activity [10]. We have

* Corresponding author. Tel.: +81 75 383 2589; fax: +81 75 383 2590.
** Corresponding author. Tel.: +81 75 383 2591; fax: +81 75 383 2592.
E-mail addresses: sanda@adv.polym.kyoto-u.ac.jp (F. Sanda), masuda@adv.polym.kyoto-u.ac.jp (T. Masuda).

0032-3861/$ - see front matter © 2007 Elsevier Ltd. All rights reserved.
doi:10.1016/j.polymer.2007.06.011

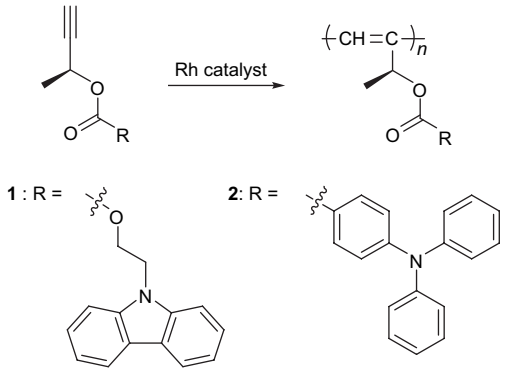

Scheme 1. Polymerization of **1** and **2**.

recently found that chiral 1-methylpropargyl alcohol serves as a powerful helical source for substituted polyacetylenes [11]. Poly(1-methylpropargyl esters) easily synthesizable from the simple alcohol take a helical structure stabilized by steric repulsion between the side chains containing chiral groups adjacent to the main chain. In the present study, we disclose the synthesis and polymerization of novel acetylene monomers substituted with carbazole and triphenylamine, and the optical and electrochemical properties, in which 1-methylpropargyl alcohol is utilized as a chiral source (Scheme 1). Although star-shaped, branched, and dendritic polymers based on triphenylamine have been extensively studied [12], the synthesis of triphenylamine-containing helical polyacetylenes has been scarcely reported so far to the best of our knowledge [13].

2. Experimental section

2.1. Measurements

^{1}H (400 MHz) and ^{13}C (100 MHz) NMR spectra were recorded on a JEOL EX-400 spectrometer using tetramethylsilane as an internal standard. IR, CD, UV–vis, and fluorescence spectra were measured on JASCO FT/IR-4100, J-820, V-550, and FP750 spectrometers, respectively. Specific rotations ($[\alpha]_D$) were measured on a JASCO DIP-1000 digital polarimeter with a sodium lamp as a light source. Melting points (m.p.) were measured on a Yanaco micromelting point apparatus. Elemental analysis was carried out at the Kyoto University Elemental Analysis Center. The number- and weight-average molecular weights (M_n and M_w) of polymers were determined by gel permeation chromatography (GPC) on a JASCO GULLIVER system (PU-980, CO-965, RI-930, and UV-1570) equipped with polystyrene gel columns (Shodex columns K804, K805, and J806) using tetrahydrofuran (THF) as an eluent at a flow rate of 1.0 mL/min, calibrated by polystyrene standards at 40 °C. Cyclic voltammograms were measured on an HCH Instruments ALS600A-n electrochemical analyzer. The measurements were carried out with a glassy carbon rod as a working electrode coupled with a Pt plate counter electrode and a Ag/AgCl reference electrode, with a solution of a polymer (1 mM) and tetrabutylammonium perchlorate (TBAP, 0.1 M) in CH_2Cl_2. UV–vis spectra of polymer films under application of voltage were measured as follows. A polymer solution (0.2 M in $CHCl_3$) was spin coated on an ITO electrode at a spin rate of 1000 rpm, and the electrode was dried under vacuum at 50 °C for 16 h. It was immersed in a solution of TBAP (0.2 M) in acetonitrile in a quartz cell. UV–vis absorption spectra of the cell were recorded under application of voltage from 0 to 2500 mV with respect to an Ag/AgCl (saturated) reference electrode. The scans of voltage were done anodically, and 5-min equilibration time was taken before each spectral scan to minimize the transient effect. The applied voltages reported herein were calibrated using ferrocene as a standard. Thermal gravimetric analysis (TGA) was carried out on a Perkin–Elmer TGA-7.

2.2. Materials

Solvents for polymerization were purified before use by the standard methods. *N*-(3-Dimethylaminopropyl)-*N*′-ethylcarbodiimide hydrochloride (EDC·HCl; Eiweiss), 4-dimethylaminopyridine (DMAP; Wako), (*S*)-(−)-3-butyn-2-ol (Aldrich),

Table 1
Polymerization of **1** and **2**[a]

Run	Monomer	Catalyst	Solvent	Yield[f] (%)	$M_n \times 10^{-3}$ [g]	M_w/M_n[g]	$[\alpha]_D$[h] (deg)
1	**1**	(nbd)Rh$^+$[η^6-$C_6H_5B^-(C_6H_5)_3$][b]	THF	86	13.0	2.03	+408
2	**1**	[Rh(nbd)Cl]–Et_3N[c]	THF	27	1.68	2.31	–[i]
3	**1**	WCl_6–Ph_4Sn[d]	Toluene	34	0.40	1.18	–[i]
4	**1**	$MoCl_5$–*n*-Bu_4Sn[e]	Toluene	25	0.73	1.36	–[i]
5	**2**	(nbd)Rh$^+$[η^6-$C_6H_5B^-(C_6H_5)_3$][b]	THF	88	15.5	3.03	+375
6	**2**	[Rh(nbd)Cl]–Et_3N[c]	THF	29	2.69	2.53	–[i]
7	**2**	WCl_6–Ph_4Sn[d]	Toluene	33	0.82	1.21	–[i]
8	**2**	$MoCl_5$–*n*-Bu_4Sn[e]	Toluene	30	0.96	1.42	–[i]

[a] $[M]_0 = 0.20$ M, 30 °C, 24 h.
[b] [Rh] = 2 mM.
[c] [Rh] = 2 mM, $[Et_3N]$ = 10 mM.
[d] $[WCl_6] = [Ph_4Sn]$ = 10 mM.
[e] $[MoCl_5] = [n\text{-}Bu_4Sn]$ = 10 mM.
[f] MeOH-insoluble part.
[g] Determined by GPC eluted with THF on the basis of polystyrene calibration.
[h] Measured by polarimetry ($c = 0.1$ g/dL, $CHCl_3$).
[i] Not determined.

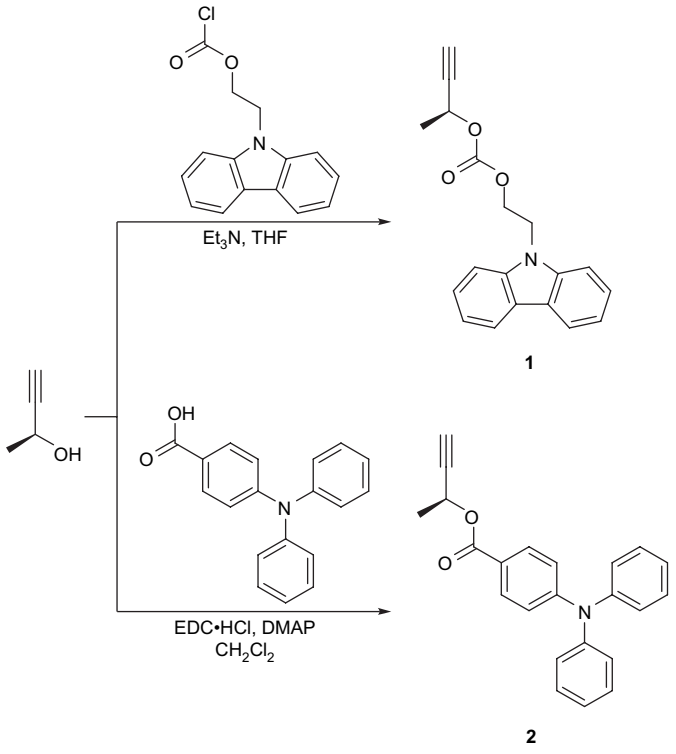

Scheme 2. Synthetic routes of **1** and **2**.

9*H*-carbazol-9-yl-ethanol (Aldrich) were purchased and used without further purification. 4-(Diphenylamino)benzoic acid was synthesized according to the literature [14]. (nbd)$Rh^+[\eta^6\text{-}C_6H_5B^-(C_6H_5)_3]$ was synthesized according to the literature [15].

2.3. Monomer synthesis

2.3.1. (*S*)-3-Butyn-2-yl 2-(9-carbazolyl)ethyl carbonate (*1*)

A 200 mL three-necked flask was equipped with a three-way stopcock and a magnetic stirring bar, and filled with dry nitrogen. A solution of 2-(9*H*-carbazol-9-yl)ethanol (2.2 g, 10.4 mmol) in THF (15 mL) was added to a solution of triphosgene (1.0 g, 3.4 mmol) in THF (30 mL). After stirring the mixture for 15 min, a solution of Et_3N (1.6 mL, 12 mmol) in THF (10 mL) was slowly added to the mixture, and the resulting mixture was stirred at room temperature overnight. Solvent-insoluble salt was filtered off to obtain a solution of 2-(9-carbazolyl)ethyl chloroformate. The solution was slowly added to a solution of (*S*)-(−)-3-butyn-2-ol (0.4 g, 5.7 mmol) in THF (12 mL) and Et_3N (2.0 mL, 14 mmol), and the resulting mixture was stirred at room temperature overnight. It was filtered, and the filtrate was concentrated on a rotary evaporator. The residual mass was purified by silica gel column chromatography eluted with *n*-hexane/ethyl acetate = 4/1 (volume ratio) to give **1** as a pale yellow solid. Yield 0.3 g (18%). M.p. 63.5–65.5 °C. $[\alpha]_D = -38°$ ($c = 0.100$ g/dL in $CHCl_3$). ^{1}H NMR (δ in ppm, $CDCl_3$): 1.43 (d, $J = 6.8$ Hz, 3H, COCH*Me*), 2.48 (s, 1H, C≡CH), 4.46–4.58 (m, 4H, CH_2CH_2N<), 5.16–5.21 (m, 1H, COC*H*Me), 7.21–7.25 (m, 2H, Ar), 7.39–7.47 (m, 4H, Ar), 8.06–8.08 (m, 2H, Ar). ^{13}C NMR (δ in ppm, $CDCl_3$): 21.0, 41.5, 64.3, 65.3, 73.9 (−C≡*C*H), 81.1 (−*C*≡CH), 108.3, 119.3, 120.3, 123.0, 125.9, 140.2, 153.9 ($-CO_2-$). IR (cm^{-1}, KBr): 3421, 3270 (≡C−H), 3046, 2989, 2121 (−C≡C−), 1747 (C=O), 1677, 1592, 1454, 1330, 1304, 1253, 1122, 1025, 890, 823, 748, 640. Anal. Calcd for $C_{19}H_{17}NO_3$: C 74.25, H 5.58, N 4.56. Found: C 74.00, H 5.35, N 4.67.

2.3.2. (*S*)- 3-Butyn-2-yl-4-(diphenylamino)benzoate (*2*)

4-(Diphenylamino)benzoic acid (1.45 g, 5.0 mmol) was added to a solution of EDC·HCl (1.0 g, 5.2 mmol) and DMAP (60 mg, 0.50 mmol) in CH_2Cl_2 (45 mL) at room temperature. (*S*)-(−)-3-Butyn-2-ol (0.40 g, 5.7 mmol) was added to the solution, and the resulting mixture was stirred at room temperature overnight. The reaction mixture was washed with water (50 mL) three times, and the organic layer was dried over anhydrous $MgSO_4$. It was filtered, and the filtrate was concentrated on a rotary evaporator. The residual mass was purified by silica gel column chromatography eluted with *n*-hexane/ethyl acetate = 4/1 (volume ratio) to give **2** as a pale yellow liquid. Yield 1.04 g (70%). $[\alpha]_D = -42.5°$ ($c = 0.100$ g/dL in $CHCl_3$). ^{1}H NMR (δ in ppm, $CDCl_3$): 1.60 (d, $J = 6.8$ Hz, 3H, COCH*Me*), 2.45 (s, 1H, −C≡CH), 5.64 (d, $J = 4.8$ Hz, 1H, COC*H*Me), 6.96–6.99 (m, 2H, Ar), 7.12–7.14 (m, 4H, Ar), 7.25–7.32 (m, 4H, Ar), 7.86–7.88 (m, 4H, Ar). ^{13}C NMR (δ in ppm, $CDCl_3$): 21.4, 60.07, 72.7 (−C≡*C*H), 82.5 (−*C*≡CH), 119.9, 121.6, 124.4, 125.8, 129.5, 131.0, 146.6, 152.2, 165.1 ($-CO_2-$). IR (cm^{-1}, KBr): 3413, 3290 (≡C−H), 3058, 2989, 2935, 2121 (−C≡C−), 1712 (C=O), 1589, 1488, 1454, 1423, 1315, 1265, 1172, 1095, 1029, 906, 848, 759, 698, 640. Anal. Calcd for $C_{23}H_{19}NO_2$: C, 80.92; H, 5.61; N, 4.10. Found: C, 80.72; H, 5.63; N, 4.12.

2.4. Polymerization

Typical procedure: All the polymerizations were carried out in a Schlenk tube equipped with a three-way stopcock under nitrogen. A THF solution of a monomer ($[M]_0 = 0.2$ M) was added to a THF solution of (nbd)$Rh^+[\eta^6\text{-}C_6H_5B^-(C_6H_5)_3]$ ($[M]_0/[cat] = 100$) under dry nitrogen, and the solution was kept at 30 °C for 24 h. The polymerization mixture was poured into a large amount of MeOH to precipitate a polymer. It was separated from the supernatant by filtration and dried under reduced pressure.

2.5. Spectroscopic data of the polymers

Poly(**1**) (run 1 in Table 1): ^{1}H NMR (δ in ppm, $CDCl_3$): 1.19–1.56 (br, 3H, OCHC*H*$_3$), 4.02 (br, 4H, COC*H*$_2$C*H*$_2$N<), 5.42 (br, 1H, OC*H*CH$_3$), 6.36 (br, 1H, −C=C*H*<), 6.95–7.78 (br, 8H, Ar); ^{13}C NMR (δ in ppm, $CDCl_3$): 20.2, 40.9, 64.6, 64.7, 108.2, 119.2, 120.2, 122.8, 125.7, 140.0, 153.8 ($-CO_2-$). IR (cm^{-1}, KBr): 3440, 3050, 2977, 1743, 1597, 1484, 1457, 1373, 1330, 1261, 1157, 1064, 1025, 871, 748, 721. Poly(**2**) (run 5 in Table 1): ^{1}H NMR (δ in ppm, $CDCl_3$): 0.80–1.60

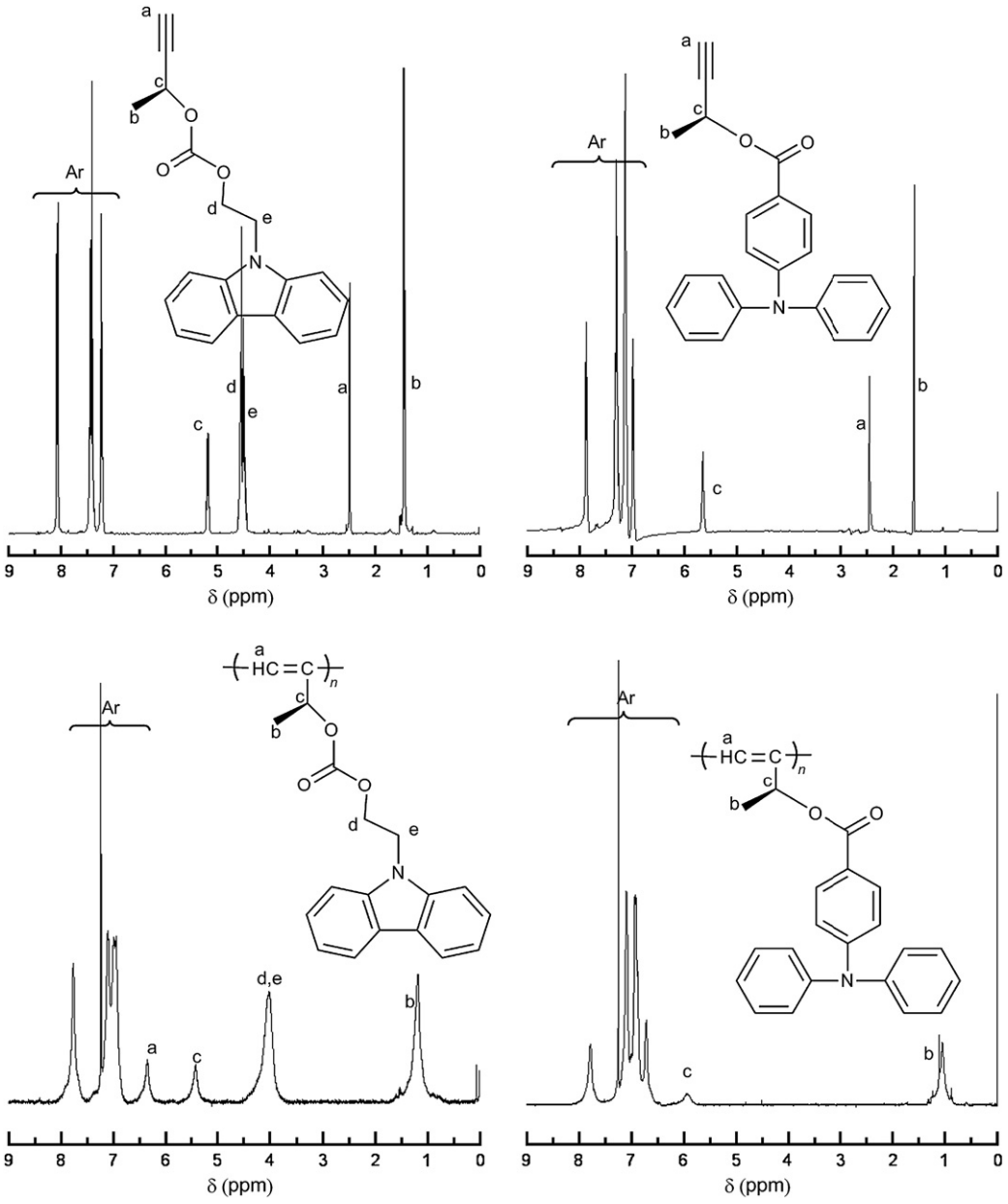

Fig. 1. ^{1}H NMR spectra (400 MHz, $CDCl_3$) of **1**, **2**, poly(**1**), and poly(**2**). Polymer samples: runs 1 and 5 in Table 1.

(br, 3H, OCHC*H*$_3$), 5.93 (br, 2H, OC*H*CH$_3$, −C═C*H*⟨), 6.71–7.78 (br, 14H, Ar).^{13}C NMR (δ in ppm, $CDCl_3$): 20.1, 60.6, 120.4, 123.0, 123.9, 125.4, 129.4, 131.1, 146.8, 151.4, 164.6 (−CO_2−). IR (cm^{-1}, KBr): 3444, 1708, 1589, 1492, 1319, 1268, 1172, 1099, 848, 755, 694.

3. Results and discussion

3.1. Monomer synthesis

Scheme 2 illustrates the synthetic routes for the carbazole- and triphenylamine-containing monomers **1** and **2**. Monomer **1** was synthesized by the reaction of (*S*)-(−)-3-butyn-2-ol with 2-(9-carbazolyl)ethyl chloroformate, which was prepared by the reaction of 2-(9-carbazolyl)ethanol with triphosgene. Monomer **2** was prepared by the condensation of the alcohol with 4-(diphenylamino)benzoic acid using EDC·HCl and DMAP as a condensation agent. The structures of the monomers were confirmed by ^{1}H, ^{13}C NMR, and IR spectra besides elemental analysis.

3.2. Polymerization

Table 1 summarizes the conditions and results of the polymerization of monomers **1** and **2** catalyzed by Rh, W, and Mo catalysts. When (nbd)Rh^{+}[η^{6}-$C_6H_5B^{-}(C_6H_5)_3$] was used (runs 1 and 5), the colorless polymerization mixture became pale yellow within 3 min, and gradually turned orange with increasing viscosity. After 24 h, the polymerization mixture was poured into a large amount of MeOH to precipitate powdery polymers [poly(**1**) and poly(**2**)] with moderate molecular weights (M_n: 13.0×10^3 and 15.5×10^3) in good yields (86

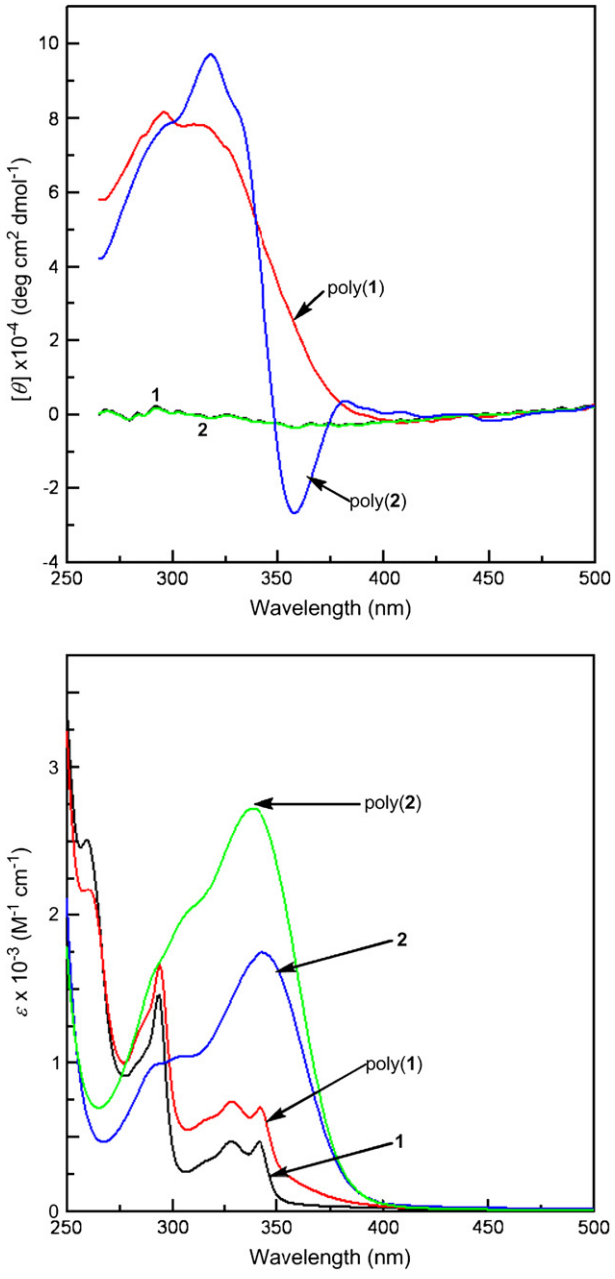

Fig. 2. CD and UV–vis spectra of **1**, **2**, poly(**1**), and poly(**2**) measured in $CHCl_3$ at 22 °C. Polymer samples: runs 1 and 5 in Table 1. [**1** and poly(**1**): $c = 3.43 \times 10^{-5}$ M, **2** and poly(**2**): $c = 2.93 \times 10^{-5}$ M].

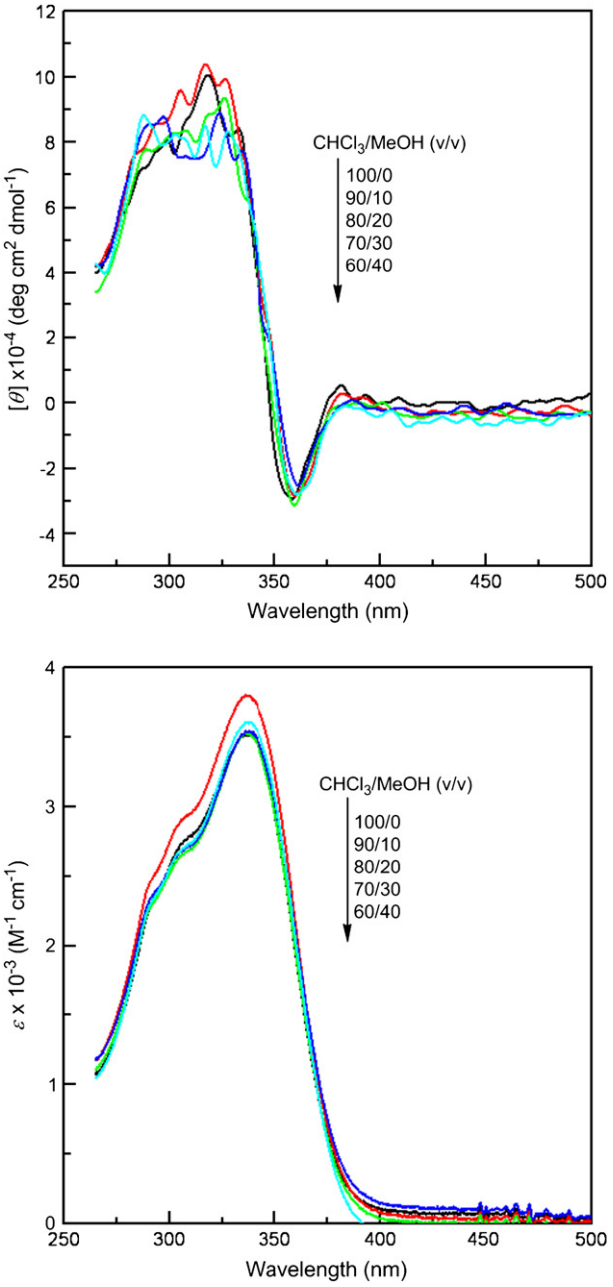

Fig. 3. CD and UV–vis spectra of poly(**2**) measured in $CHCl_3$/MeOH ($c = 2.93 \times 10^{-4}$ M) with various compositions (100/0–60/40, v/v) at 22 °C. Polymer sample: run 5 in Table 1.

and 88%). The polymers were completely soluble in CH_2Cl_2, $CHCl_3$, toluene, THF, and insoluble in acetone, MeOH, diethyl ether, and *n*-hexane. Interestingly, $[(nbd)RhCl]_2$–Et_3N gave low-molecular-weight polymers (runs 2 and 6). We also polymerized the monomers using $MoCl_5$–*n*-Bu_4Sn and WCl_6–Ph_4Sn as catalysts to obtain only low-molecular-weight oligomers ($M_n < 1 \times 10^3$) (runs 3, 4, 7, and 8).

3.3. Polymer structure

The polymer structures were examined by IR and ^{1}H NMR spectroscopies. The monomers exhibited IR absorption bands around 3280 and 2121 cm^{-1} associated with the ≡C–H and –C≡C– stretching vibrations, respectively, while the polymers did not exhibit these peaks. Accordingly, the polymers displayed no ^{1}H NMR signal around 2.45 ppm assignable to an acetylenic proton as shown in Fig. 1. In the ^{13}C NMR spectra, the polymers displayed no signals assignable to ethynyl carbons around 73 and 81–83 ppm. All these results clearly indicate that the acetylene polymerization took place to form polymers composed of alternating single and double bonds. The *cis* content of the main chain of poly(**1**) was 86%, which was determined by the integration ratio of *cis* vinyl proton and the other proton signals, while that of poly(**2**) could not be determined, because the signals appeared very broadly, and the

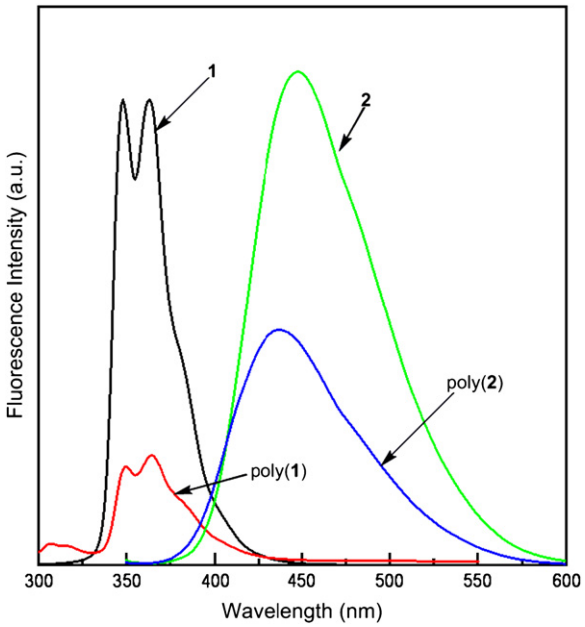

Fig. 4. Fluorescence spectra of **1**, **2**, poly(**1**), and poly(**2**) measured in $CHCl_3$ at 22 °C excited at 294 nm [**1** and poly(**1**): $c = 3.43 \times 10^{-6}$ M] and 343 nm [**2** and poly(**2**): $c = 2.93 \times 10^{-6}$ M]. Polymer samples: runs 1 and 5 in Table 1. The intensities are normalized based on the concentration of carbazole unit.

signals assignable to the olefinic proton of the polyacetylene main chain overlapped with aromatic proton signals. Since Rh catalysts predominantly afford polyacetylenes with *cis* structure, it is assumed that the steric structure of poly(**2**) in the present study is also the case.

3.4. Secondary structure of the polymers

The secondary structures of the polymers were examined by polarimetry, CD and UV–vis spectroscopies. Table 1 lists the $[\alpha]_D$ values of poly(**1**) and poly(**2**) measured in $CHCl_3$. In contrast to **1** ($[\alpha]_D = -38°$, $c = 0.100$ g/dL in $CHCl_3$ at room temperature), poly(**1**) displayed large plus optical rotations, which suggests that it took a helical structure with a predominantly one-handed screw sense. Similarly, poly(**2**) also seemed to form a helix with an excess of one-handedness in $CHCl_3$ on the basis of the large $[\alpha]_D$ compared to that of **2** ($[\alpha]_D = -42.5°$, $c = 0.100$ g/dL in $CHCl_3$ at room temperature). We also examined the $[\alpha]_D$ of poly(**1**) and poly(**2**) in THF, toluene, and CH_2Cl_2 to find that the $[\alpha]_D$ slightly changed with solvents.

The top part of Fig. 2 shows the CD spectra of poly(**1**) and poly(**2**) measured in $CHCl_3$. Although monomers **1** and **2** were CD inactive, poly(**1**) showed a strong CD signal at 294 nm, and poly(**2**) exhibited large plus and minus signals at 325 and 360 nm, respectively. It is unambiguously testified that the polymer adopted a helical conformation with a preferred screw sense. In the UV–vis spectra, the polymers exhibited the absorption patterns similar to the corresponding monomers as shown in the bottom part of Fig. 2. The larger intensities of UV–vis absorption of polymers are attributable to the partial overlap of the absorption peaks based on the side chain chromophors with those of the polyacetylene backbone. Judging from the peak top differences between the UV–vis and CD spectra of the polymers, it seems that the helical polyacetylene main chain mainly induces the Cotton effects.

The temperature dependence of the CD and UV–vis spectra of poly(**1**) and poly(**2**) was examined. When the measuring temperature was raised from −10 to 50 °C in $CHCl_3$, the magnitude of Cotton effect only slightly changed (not shown). We also measured the CD and UV–vis spectra of poly(**1**) and poly(**2**) at a temperature in the range from −10 to 100 °C in toluene to find the slight change of Cotton effect, which was similar to that in $CHCl_3$. It was considered that the helical structure of the polymers was thermally very stable at this temperature range. The tolerance of the helicity to heat of the present polymers is remarkably high among helical polyacetylenes, which commonly transform into random coil at this high temperature [16]. One possible reason for this is the rigidity of the polymer chain enhanced by the methyl group in the immediate neighborhood of the polyene backbone.

When helical structures of polyacetylenes are stabilized by the support of intramolecular hydrogen bonding like poly(*N*-propargylamides), they transform into random coil by the addition of polar solvent such as MeOH due to collapse of the regulated hydrogen bonding strands. Since the present polymers are not the case, they are predicted to be stable to polar solvents. In fact, almost the same CD spectrum irrespective of $CHCl_3$/MeOH composition clearly shows that the helical structure is very stable against polar solvents (Fig. 3).

3.5. Fluorescence properties

Fig. 4 shows the fluorescence spectra of poly(**1**) and poly(**2**) along with the monomers. The solutions of **1** and **2** emitted luminescence at 375 and 460 nm with fluorescence quantum yields (ϕ) of 23% and 77% upon excitation at 294 and 343 nm, which should come from carbazole and triphenylamine, respectively. Poly(**1**) and poly(**2**) emitted fluorescence in a manner similar to **1** and **2**, while the ϕ values of the polymers were much smaller than those of the corresponding monomers [poly(**1**) 0.5%, poly(**2**) 7.2%]. The polyacetylene backbone possibly works as a quenching site for light emission, which absorbs the light emitted from the appendages with the energy dissipated via nonradiative decay, thus resulting in low photoluminescence efficiency of the polymers.

3.6. Electrochemical properties

Fig. 5 depicts the cyclic voltammetric (CV) curves of poly(**1**) and poly(**2**) together with **1** and **2**. The oxidation of poly(**1**) initiated at 0.84 V in the first cycle, which was somewhat lower than that of **1** (1.03 V). This result may indicate that carbazole moieties of the polymer synergize with the polyacetylene main chain, resulting in high electron density at the nitrogen atom compared to that of the monomer. As the CV scans continued, poly(**1**) exhibited two oxidation peaks in the region of 0.63–0.84 V, one of which was absent in the first

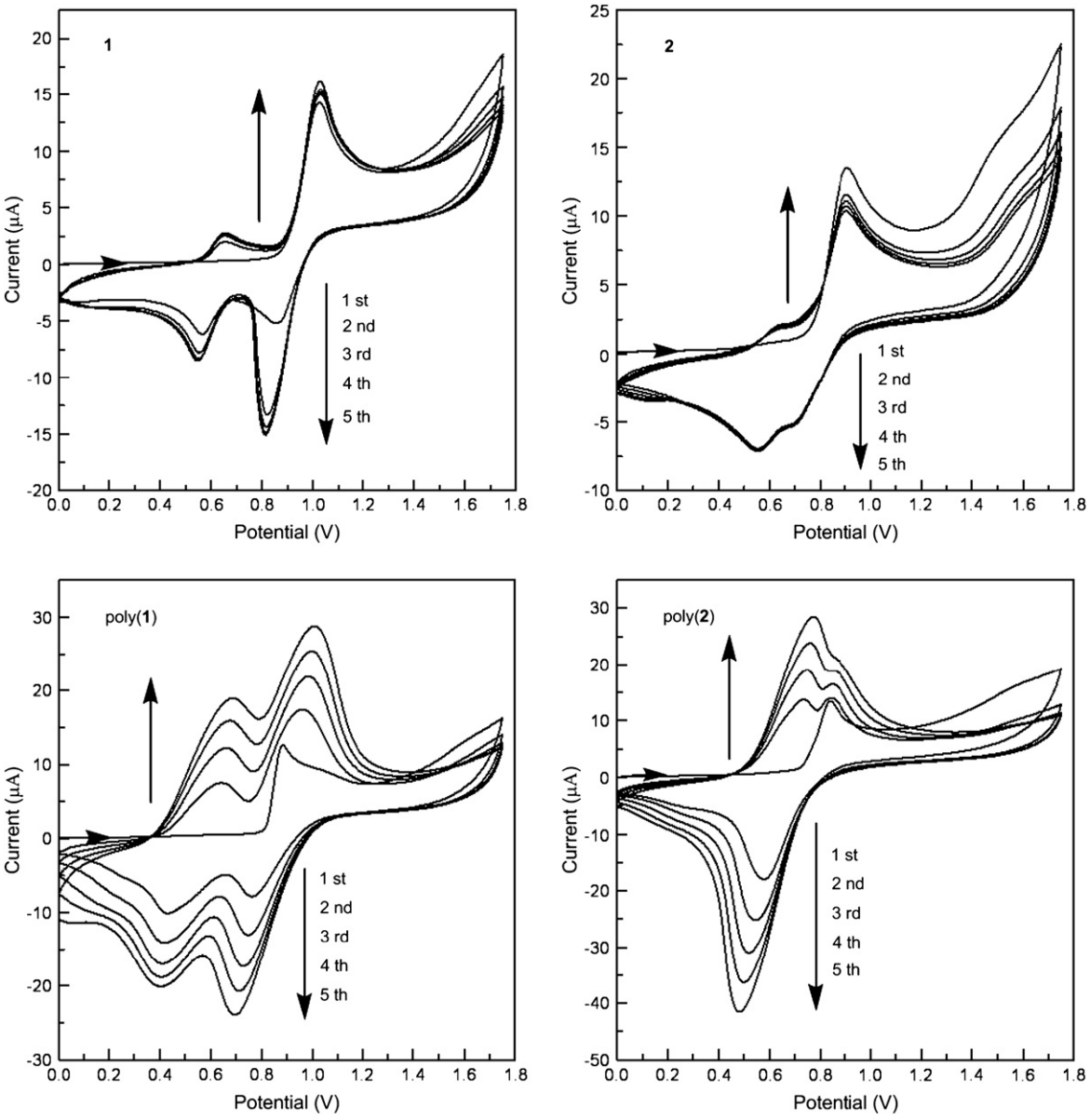

Fig. 5. Cyclic voltammograms of **1**, **2**, poly(**1**), and poly(**2**) measured at a scan rate of 0.1 V/s vs Ag/Ag^+ in a solution of TBAP (0.2 M) in CH_2Cl_2. Polymer samples: runs 1 and 5 in Table 1.

cycle. It seems that the pendent carbazole moieties were oxidized in the first scan, followed by irreversible formation of dicarbazyls [17]. The peaks shifted to a higher potential field as the CV scans continued. It seems that a conducting polymer film was formed on the working electrode surface, and the film thickness gradually increased upon CV scanning. The potential shift of this maximum provided the information about the increase of the electrical resistance in the polymer film; over-potential was needed to overcome the resistance. It exhibited two reduction peaks in the region of 0.43 − 0.76 V.

The oxidation of poly(**2**) started at 0.84 V in the first scan, which was lower than that of **2** showing a stepwise-oxidation wave at 0.91 V. Poly(**2**) showed an oxidation peak around 0.74 V and the corresponding reduction peak was around 0.55 V. The oxidation and reduction potentials of poly(**2**) gradually shifted to positive and negative fields as the scans continued, respectively, in a manner similar to the case of poly(**1**).

3.7. Electrochromism

Fig. 6 depicts the CD and UV−vis spectra of films of poly(**1**) and poly(**2**) fabricated by spin coating. The films of poly(**1**) and poly(**2**) changed the color from pale yellow to pale blue by application of voltage. The polymer film kept blue color after stopping voltage application. The electrochromic process was irreversible. Before electric potential was applied, the film of poly(**2**) showed plus- and minus-signed CD signals at 330 and 360 nm, respectively, similar to that of solution state as shown in Fig. 2. Poly(**2**) should also take

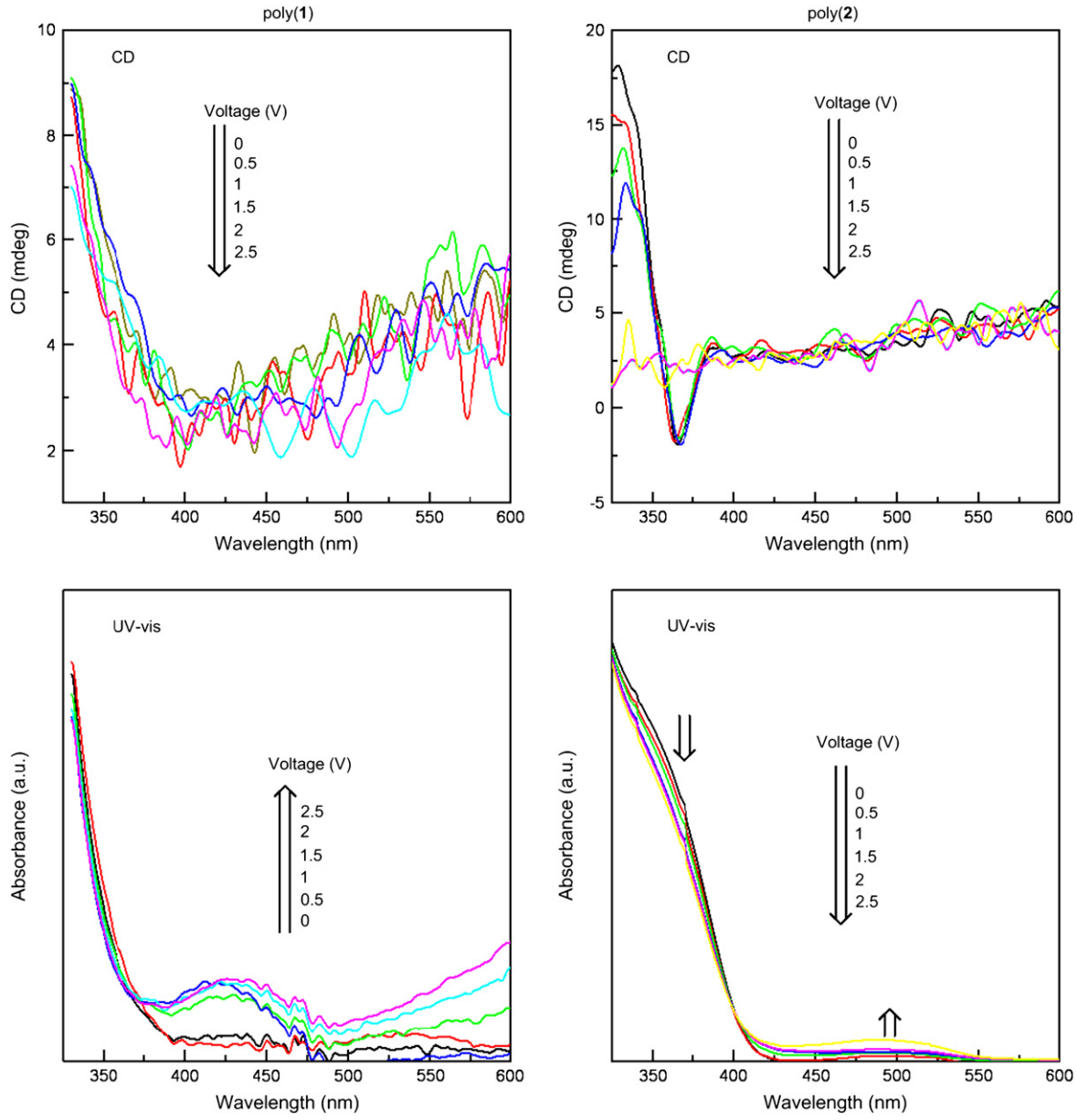

Fig. 6. UV–vis spectra of films of poly(**1**) and poly(**2**) fabricated on an ITO electrode under application of voltage. Polymer samples: runs 1 and 5 in Table 1.

a helical structure in the film state. The plus CD signal at 330 nm gradually decreased the intensity by applying voltage, and completely disappeared at 2 V. Simultaneously, the UV–vis shoulder peak decreased the intensity. It is assumed that the helical structure transformed into a random coil conformation. At the same time, an absorption peak appeared around 500 nm and increased the intensity. It is speculated that the peak is derived from a polaron formed at the triphenylamine moiety [18]. On the other hand, poly(**1**) exhibited the UV–vis spectroscopic change based on polaron formation, but no change of CD signal upon application of voltage.

3.8. Thermal properties

Fig. 7 depicts the TGA traces of the polymers. The onset temperatures of weight loss of poly(**1**) and poly(**2**) were 225 and 270 °C under air, respectively. Poly(**2**) was thermally more stable than poly(**1**). The ester linkage of poly(**2**) seems to be more stable than the carbonate of poly(**1**). The presence of a planar region around 400 °C suggests that the thermolysis of the polymers initially occurs at the carbonate and ester linkage to release the carbazole and triphenylamine moieties in the early stage, then the decomposition of the polyacetylene backbone takes place. They completely lost their weights around 500 °C.

4. Conclusions

In this study, we have synthesized acetylene derivatives **1** and **2** bearing carbazole and triphenylamine moieties, and polymerized them to obtain poly(**1**) and poly(**2**) with moderate molecular weights in good yields. The polymers took a helical

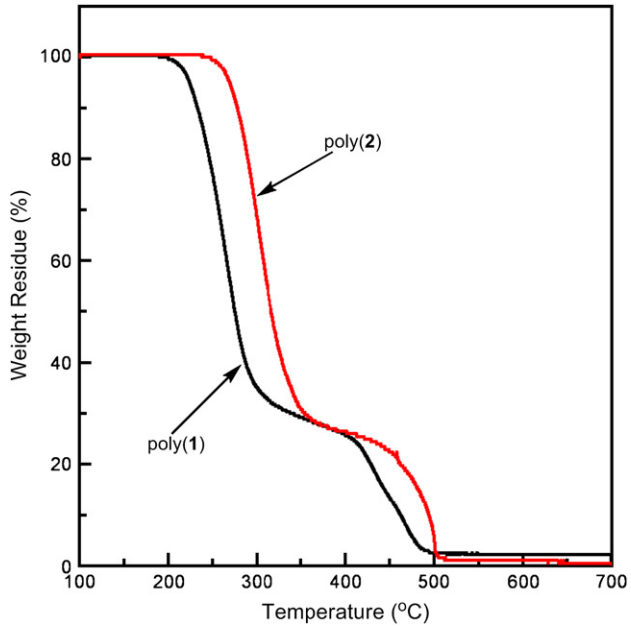

Fig. 7. TGA curves of poly(**1**) and poly(**2**) measured at a heating rate of 10 °C/min in air. Polymer samples: runs 1 and 5 in Table 1.

conformation with predominantly one-handed screw sense, exhibiting large molar ellipticities based on the helical polyacetylene backbone. The helical structure of the polymers was very stable against heating and addition of MeOH. The polymers changed the color from pale yellow to blue by application of voltage, presumably caused by the formation of a polaron at the carbazole and triphenylamine moieties. These polymers were stable below 225–270 °C under air, and then decomposed to lose weight around 500 °C completely.

Acknowledgments

This research was partly supported by a Grant-in-Aid for Science Research in a Priority Area "Super-Hierarchical Structures (no. 446)" from the Ministry of Education, Culture, Sports, Science and Technology, Japan. Jinqing Qu acknowledges the financial support from the Ministry of Education, Culture, Sports, Science, and Technology (Monbukagakusho), Japan.

References

[1] (a) Grazulevicius JV, Strohriegl P, Pielichowski J, Pielichowski K. Prog Polym Sci 2003;28:1297;
(b) Wang YZ, Epstein AJ. Acc Chem Res 1999;32:217.
[2] (a) Tang BZ, Chen HZ, Xu RS, Lam JWY, Cheuk KKL, Wong HNC, et al. Chem Mater 2000;12:213;
(b) Pui-Sze Lee P, Geng Y, Kwok HS, Tang BZ. Thin Solid Films 2000;363:149.
[3] (a) Tabata M, Fukushima T, Sadahiro Y. Macromolecules 2004;37:4342;
(b) Brizius G, Kroth S, Bunz UHF. Macromolecules 2002;35:5317;
(c) Percec V, Obata M, Rudick JG, De BB, Gloode M, Bera TK, et al. J Polym Sci Part A Polym Chem 2002;40:3509;
(d) Roh Y, Bauld NL. Adv Synth Catal 2002;2:192;
(e) Gao D, Roh Y, Bauld NL. Adv Synth Catal 2001;343:269;
(f) Gratt J, Cohen RE. Macromolecules 1997;30:3137;
(g) Finkelshtein ES, Portnyk EB, Ushakov NV, Greengolts ML, Fedorova GK, Platé NA. Macromol Chem Rapid Commun 1994;15:155;
(h) Park JW, Lee JH, Cho HN, Choi SK. Macromolecules 1993;26:1191.
[4] (a) Qu J, Kawasaki R, Shiotsuki M, Sanda F, Masuda T. Polymer 2006;47:6551;
(b) Fulghum T, Abdul Karim SM, Baba A, Taranekar P, Nakai T, Masuda T, et al. Macromolecules 2006;39:1467;
(c) Sanda F, Nakai T, Kobayashi N, Masuda T. Macromolecules 2004;37:2703;
(d) Sanda F, Kawasaki R, Shiotsuki M, Masuda T. Polymer 2004;45:7831;
(e) Sanda F, Kawaguchi T, Masuda T. Macromolecules 2003;36:2224;
(f) Sata T, Nomura R, Wada T, Sasabe H, Masuda T. J Polym Sci Part A Polym Chem 1998;36:2489;
(g) Nakano M, Masuda T, Higashimura T. Polym Bull 1995;34:191.
[5] (a) Masuda T. J Polym Sci Part A Polym Chem 2007;45:165;
(b) Jack W, Lam Y, Tang BZ. Acc Chem Res 2005;38:745;
(c) Masuda T, Sanda F, Shiotsuki M. In: Crabtree RH, Mingos DMP, editors. Comprehensive organometallic chemistry III. Oxford: Elsevier; 2007 [chapter 11.16];
(d) Masuda T, Sanda F. In: Grubbs RH, editor. Handbook of metathesis, vol. 3. Weinheim: Wiley-VCH; 2003 [chapter 3.11].
[6] (a) Nakano T, Okamoto Y. Chem Rev 2001;101:4013;
(b) Okamoto Y, Nakano T. Chem Rev 1994;94:349.
[7] (a) Sanda F, Araki H, Masuda T. Chem Lett 2005;34:1642;
(b) Yashima E, Maeda K, Okamoto Y. Polym J 1999;31:1033.
[8] (a) Qu J, Kawasaki R, Shiotsuki M, Sanda F, Masuda T. Polymer 2007;48:467;
(b) Sanda F, Kawasaki R, Shiotsuki M, Masuda T. Macromol Chem Phys 2007;208:765.
[9] Qu J, Shiotsuki M, Sanda F, Masuda T. Macromol Chem Phys 2007;208:823.
[10] Zhao H, Sanda F, Masuda T. J Polym Sci Part A Polym Chem 2007;45:253.
[11] Suzuki Y, Shiotsuki M, Sanda F, Masuda T. Macromolecules 2007;40:1864.
[12] (a) Thelakkat M. Macromol Mater Eng 2002;287:442;
(b) Bernius MT, Inbasekaran M, O'Brien J, Wu WS. Adv Mater 2000;12:1737;
(c) Shirota Y. J Mater Chem 2000;10:1.
[13] Murata H, Miyajima D, Nishide H. Macromolecules 2006;39:6331.
[14] Behl M, Zentel R, Broer DJ. Macromol Rapid Commun 2004;25:1765.
[15] Schrock RR, Osborn JA. Inorg Chem 1970;9:2339.
[16] (a) Tabei J, Nomura R, Sanda F, Masuda T. Macromolecules 2004;37:1175;
(b) Tabei J, Nomura R, Sanda F, Masuda T. Macromolecules 2003;36:8603;
(c) Nomura R, Yamada K, Tabei J, Takakura Y, Takigawa T, Masuda T. Macromolecules 2003;36:6939;
(d) Tabei J, Nomura R, Masuda T. Macromolecules 2003;36:573;
(e) Nomura R, Tabei J, Nishiura S, Masuda T. Macromolecules 2003;36:561;
(f) Tabei J, Nomura R, Masuda T. Macromolecules 2002;35:5405.
[17] Park JW, Lee JH, Ko JM, Cho HN, Choi SK. J Polym Sci Part A Polym Chem 1994;32:2789.
[18] (a) Wei ZH, Xu JK, Nie GM, Du YK, Pu SZ. J Electroanal Chem 2006;589:112;
(b) Chiu KY, Su TX, Li JH, Lin TH, Liou GS, Cheng SH. J Electroanal Chem 2005;575:95.